Molecular dynamics simulation of cross-slip and the intersection of dislocations in copper

2003 J. Phys.: Condens. Matter 15 3391

(http://iopscience.iop.org/0953-8984/15/20/303)

INSTITUTE OF PHYSICS PUBLISHING JOURNAL OF PHYSICS: CONDENSED MATTER

J. Phys.: Condens. Matter **15** (2003) 3391–3399 PII: S0953-8984(03)55726-5

Molecular dynamics simulation of cross-slip and the intersection of dislocations in copper

M Li, W Y Chu, K W Gao and L J Qiao

Department of Materials Physics, University of Science and Technology, Beijing 100083, China

E-mail: mlik33@yahoo.com

Received 7 November 2002
Published 12 May 2003
Online at stacks.iop.org/JPhysCM/15/3391

Abstract

The molecular dynamics method is used to simulate cross-slip by thermal activation at 30 K and the intersection of dislocations in copper containing 1.6×10^6 atoms using the embedded atom method potential. The results show that an extended screw dislocation can recombine through thermal activation at 30 K into a constriction on the surface because of stress imbalance and the constriction will split again in the other slip plane. Removing the constriction along the extended dislocation results in a cross-slip of the screw dislocation at low temperature. After the intersection between a moving right-hand screw dislocation DC and a perpendicular left-hand dislocation BA, whose ends are fixed on the surfaces, an extended jog corresponding to a row of one-third vacancies forms in BA and a trail of vacancies behind DC. If the intersected dislocation is a right-hand screw dislocation AB, the jog formed in AB corresponds to a row of one-third interstitials and the point defects behind DC are interstitials. After the intersection between screw and edge dislocations, the jog formed in the edge dislocation corresponds to a row of one-third vacancies and there are no point defects behind the screw dislocation.

(Some figures in this article are in colour only in the electronic version)

1. Introduction

The elasticity theory of dislocations has proved successful in explaining a broad variety of dislocation behaviours [1]. The core region of dislocations and their interactions where the linear elasticity assumption fails, however, is still the subject of extensive research. The atomic level core structures of dislocations in single crystalline gold and iridium have been studied using high-resolution electron microscopy (HREM) [2]. Atom positions and local structure around a perfect dislocation and the central stacking fault of a z-shaped faulted dipole in deformed GaAs have been evaluated numerically through HREM analysis [3]. Much work has been carried out concerning atomistic simulations of the dislocation core [4–10]. For example,

the pressure-dependent core properties of screw dislocation in Ta have been simulated by means of quantum-based, multi-ion inter-atomic potentials derived from model generalized pseudo-potential theory [4]. The core width, energy and Peierls stress for different dislocations have been investigated using first-principles density functional theory [5]. Dislocation cross-slip in copper and nickel has been simulated using the nudged elastic band method and inter-atomic potentials based on the effective-medium theory [6].

Dislocation emission, crack propagation and healing can be simulated by a molecular dynamics method [7, 8]. The intersection process between a screw dislocation and a 60° dislocation has also been simulated by the molecular dynamics method [8]. The annihilation process of screw dislocations has been simulated and it was found that dislocations do not split into partials if their separation is less than a certain distance [10]. Molecular dynamics simulation of a supersonic dislocation has been performed [11].

Up to now, however, the possibility of dislocation cross-slip through thermal activation at extremely low temperature and the details of an extended jog formed after dislocation intersections have not been investigated. In the present paper, a molecular dynamics method is used to simulate dislocation cross-slip at 30 K and to investigate in detail some extended jogs formed after the intersection of various dislocations in copper.

2. Simulation procedure

In our super-cell, the length of copper crystal along the $x = [1\bar{1}\bar{2}]$ direction is 31.2 nm, the width along the $y = [1\bar{1}1]$ direction is 21 nm and the height along the $z = [110]$ direction is 25.8 nm. The number of atoms used here is about 1.6×10^6. The inter-atomic potential used here is the embedded atom method (EAM) [11]. The inner atoms follow Newton's second law and a leapfrog algorithm is applied to calculate the positions and velocities of atoms [11]. The initial velocity is the Maxwell–Boltzmann distribution corresponding to a given temperature, which is maintained at 30 K during simulations.

Dislocations are implemented by displacing the position of each atom with a displacement field according to the linear elasticity theory of dislocations and then relaxing the system for 1.0 ps. The potential energy of all lattice atoms is distributed between −3.55 and −3.51 eV and energy of the atoms around the dislocation core is distributed between −3.49 and −3.45 eV, which is higher than that of the lattice atoms. These atoms with their energy distributions are distinguished by different shades of colours. Therefore, the positions of the dislocations at any instant can be identified. When the temperature exceeds 200 K, the energy distribution of the lattice atoms widens greatly and overlaps with that of the dislocation core. In this case, the site of the dislocation line cannot be determined according to the energy distribution, i.e. the colour of atoms. In this paper, the system temperature is maintained at 30 K by scaling the atom velocities during the simulation. Thompson tetrahedron notation is used to mark Burger's vectors and slip planes.

3. Results and discussion

3.1. Cross-slip through thermal activation at 30 K

The free boundary condition is used. A screw dislocation QP in the $(1\bar{1}1)$ plane with $\boldsymbol{b} = DC = [110]/2$ is implemented by displacing the position of each atom with a displacement field according to elasticity theory [1]. After free relaxation of the computational cell for 1.0 ps, the dislocation dissociates into an extended dislocation consisting of two Shockley partials $\boldsymbol{D\alpha}$ and $\boldsymbol{\alpha C}$ in the $(\bar{1}11)$ plane, as shown in figure 1(a). The equilibrium separation between the partials measured, based on figure 1(a), is $r_e = 1.88$ nm. The equilibrium separation according

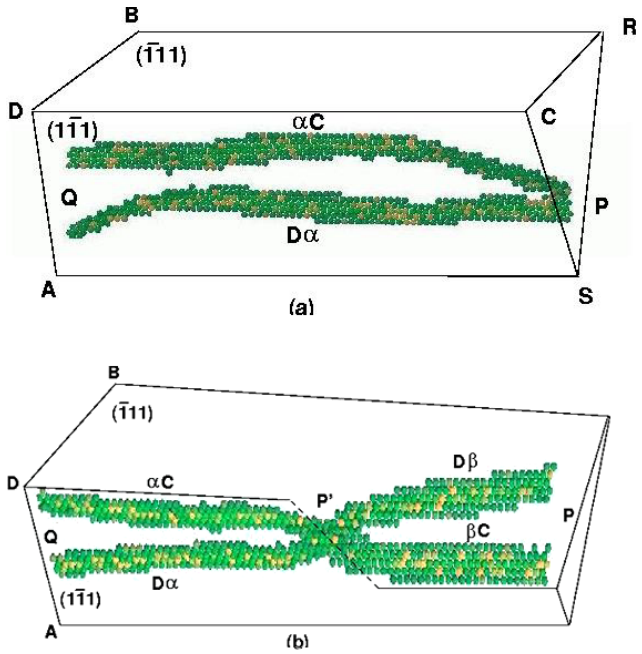

Figure 1. Cross-slip of a screw dislocation via thermal activation at 30 K, (a) the extended dislocation $D\alpha + \alpha C$ recombines into a constriction P on the surface SCR, (b) the constriction P is split again on the new slip plane of $(\bar{1}11)$ and the constriction P moves to P'.

to isotropy elasticity theory is given by [1]

$$r_e = \frac{\mu b_1^2(2-\nu)}{8\pi\gamma(1-\nu)}\left(1 - \frac{2\nu\cos 2\theta}{2-\nu}\right). \tag{1}$$

where μ is the shear modulus, $\boldsymbol{b}_1 = [21\bar{1}]/6$ is the Burger's vector of the partial, ν is the Poisson ratio, γ is the stacking fault energy and $\theta = 0$ for the screw dislocation. Substituting the data of copper shown in [1], the equilibrium separation calculated based on equation (1) is $r_e = 1.6$ nm. Similarly, the equilibrium separation calculated according to anisotropy elasticity theory [1] is $r_e^* = 0.98$ nm. The simulation result is closer to the value calculated by isotropic elasticity theory than to that from anisotropic theory because the isotropic elasticity constants were used in constructing the EAM potential.

The partials vibrate during relaxation because of thermal activation and the extended dislocation may recombine into a constriction P at the surface SCR because of stress imbalance on the surfaces, as shown in figure 1(a). The constriction P is a perfect dislocation that can be split into $\boldsymbol{D\beta} + \boldsymbol{\beta C}$ again on the new slip plane $(\bar{1}11)$. Through thermal activation, the constriction P can move along the dislocation line to site P'. As a result, the dislocation located at the right of P' is split on the $(\bar{1}11)$ plane and that at the left of P' is split on the $(1\bar{1}1)$ plane, as shown in figure 1(b). The motion of the constriction by thermal activation at 30 K makes the extended dislocation on the slip plane $(1\bar{1}1)$ split step by step on to the other slip plane $(\bar{1}11)$. At last, the dislocation $\boldsymbol{DC}$ can cross-slip completely from the $(1\bar{1}1)$ plane to the $(\bar{1}11)$ plane only through thermal activation at 30 K. The recombination of a constriction on the free surface due to stress imbalance seems a key-point in the understanding of cross-slip through thermal activation at extreme low temperatures.

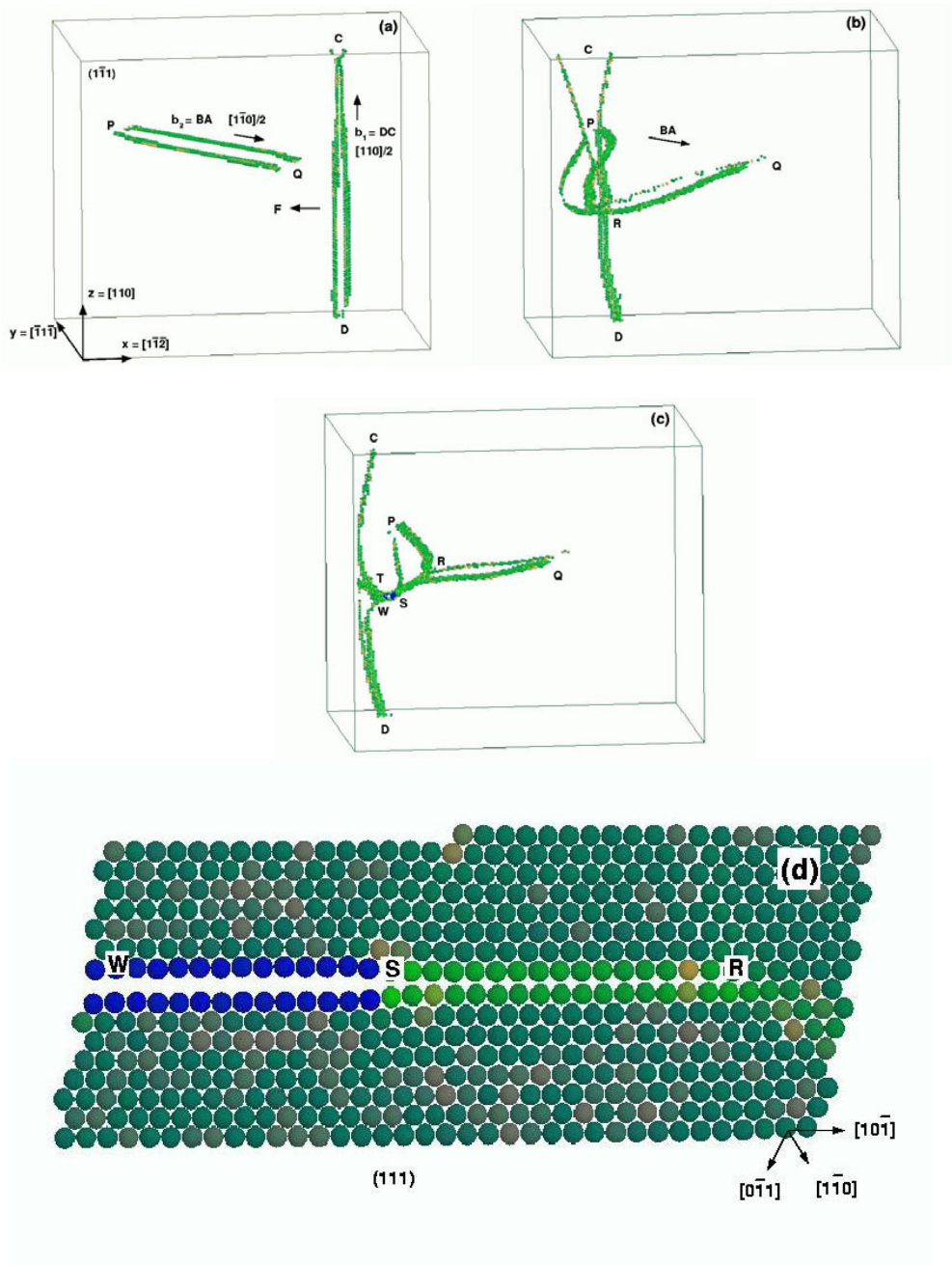

Figure 2. Intersection between perpendicular screw dislocations, (a) the right-hand dislocation DC moving along the [$\bar{1}$12] direction and the ends of Q and P of the left-hand dislocation BA fixed on the surfaces, (b) intersection of these two dislocations at point R, (c) an extended jog RS in BA and a trail of vacancies SW left behind DC after intersection, (d) the atomic configuration around the vacancies SW and the jog RS in the (111) plane.

3.2. Dislocation intersections

The fixed boundary condition on the front and back surfaces, i.e. the $(1\bar{1}1)$ planes, and the free boundary condition on all other surfaces are used. A right-hand screw dislocation $\boldsymbol{DC}$ on the (111) plane is forced to move to the left as shown in figure 2(a). The ends of a left-hand screw dislocation $\boldsymbol{BA}$ on the $(1\bar{1}1)$ plane are fixed on the front and back surfaces because of the fixed boundary condition. A shear stress τ_{zy} on the $(1\bar{1}1)$ plane is applied with a loading rate of 334 MPa ps^{-1}. This shear stress produces the Peach–Koehler force to move the dislocation $\boldsymbol{DC}$. The time step is 5×10^{-3} ps. The stress is increased to 1.34 GPa, corresponding a strain of 2.53%, and then kept constant. The dislocation $\boldsymbol{DC}$ moves along the $[\bar{1}12]$ direction with a maximum velocity of 1.6×10^3 m s^{-1}, which is about 2/3 of the transverse sound wave speed for copper. The force between these two perpendicular dislocations is repulsive, according to elasticity theory. As the two dislocations approach each other, the repulsive force reaches a maximum so the dislocation lines no longer stay straight. The pinned partials $\boldsymbol{B}\delta$ and $\delta\boldsymbol{A}$ show a prominent curvature. The partials $\boldsymbol{D}\alpha$ and $\alpha\boldsymbol{C}$ gradually move close to each other and form a compact core configuration while they are approaching the dislocation $\boldsymbol{BA}$. The moving dislocation $\boldsymbol{DC}$ and the pinned dislocation $\boldsymbol{BA}$ intersect at R, as shown in figure 2(b). At the time of intersection, the compactness of $\boldsymbol{DC}$ remains, whereas $\boldsymbol{BA}$ keeps its dissociation as $\boldsymbol{B}\delta$ and $\delta\boldsymbol{A}$. $\boldsymbol{DC}$ passes $\boldsymbol{B}\delta$ and $\delta\boldsymbol{A}$ one after another. An extended jog RS in $\boldsymbol{BA}$ and a trail of point defects SW are left behind $\boldsymbol{DC}$ after intersection, as shown in figure 2(c). At first, the trail of point defects is coplanar with the jog RS and both are located on the (111) plane. When the dislocation $\boldsymbol{DC}$ moves continuously forward, the trail of point defects deviates from the (111) plane. The atomic configuration of the extended jog RS and the coplanar trail of the point defects SW in the (111) plane are shown in figure 2(d). We can see that the trail of the point defects SW is a row of vacancies and the extended jog is a hollow tube, whose volume is about one-third of a row of vacancies.

When the intersected screw dislocation $\boldsymbol{AB}$ is a right-hand dislocation instead of a left-hand dislocation, the intersection process is similar to that shown in figure 2. There is also an extended jog EF created in the intersected dislocation $\boldsymbol{AB}$ on the (111) plane. A trail of point defects FG is left behind the moving dislocation $\boldsymbol{DC}$. This trail of point defects is located on the $(1\bar{1}1)$ plane after intersection, as shown in figure 3(a). The atomic configuration around the trail of the point defects FG in the $(1\bar{1}1)$ plane is shown in figure 3(b). As viewed along the atomic row of $abcd$, we can see that the arrangement of the atoms in the region of bc is closer together than that of ab and cd. This means that there is an interstitial in the region of bc. The situation is the same in the whole zone of FG. Therefore, the trail of the point defects after intersection between a perpendicular pair of right-hand screw dislocations is a row of interstitials. The atomic configuration around the extended jog EF on the (111) plane is shown in figure 3(c). As viewed along the atomic row of $abcd$, the arrangement of the atoms in the region of bc is closer together than that of ab or cd. Therefore, the extended jog EF in the right-hand screw dislocation $\boldsymbol{AB}$ is composed of interstitials, however, its volume cannot be determined according to figure 3(c).

If the intersected dislocation is an edge dislocation $\boldsymbol{CB} = [\bar{1}01]/2$ on the (111) plane, an extended jog RS forms in $\boldsymbol{CB}$, as shown in figure 4(a). The atomic configuration around the jog RS on the (111) plane is shown in figure 4(b). Comparing figure 4(b) with figure 2(d), we can see the jog in the edge dislocation is also a hollow tube and its volume is also about one-third of a row of vacancies. There are no point defects left behind the moving dislocation $\boldsymbol{DC}$ because a kink instead of a jog is created in $\boldsymbol{DC}$ after intersection, which disappears through slip motion on the $(1\bar{1}1)$ plane.

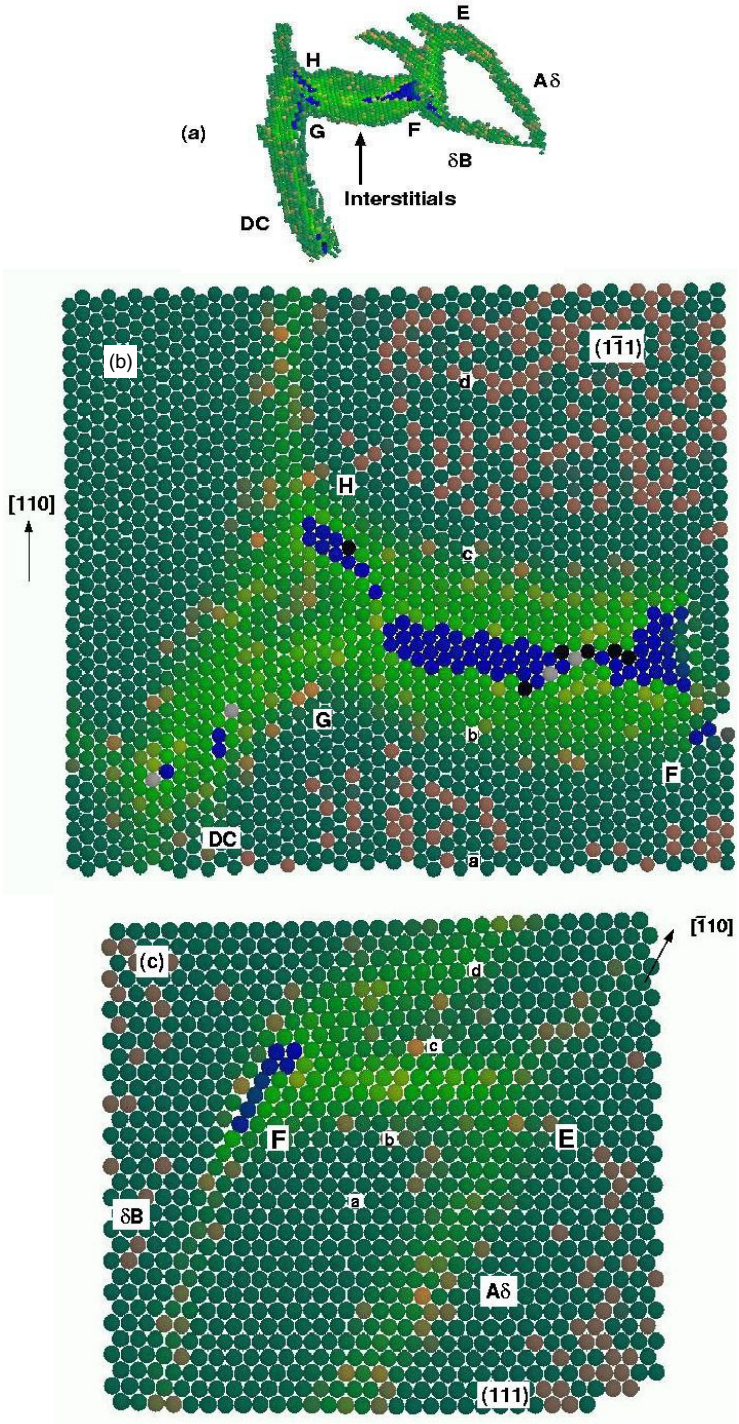

Figure 3. Intersection between a pair of perpendicular right-hand screw dislocations, (a) an extended jog EF in AB and a trail of point defects FG behind DC after intersection, (b) the atomic configuration around the trail FG in the (1$\bar{1}$1) plane, (c) the atomic configuration around the jog EF in the (111) plane.

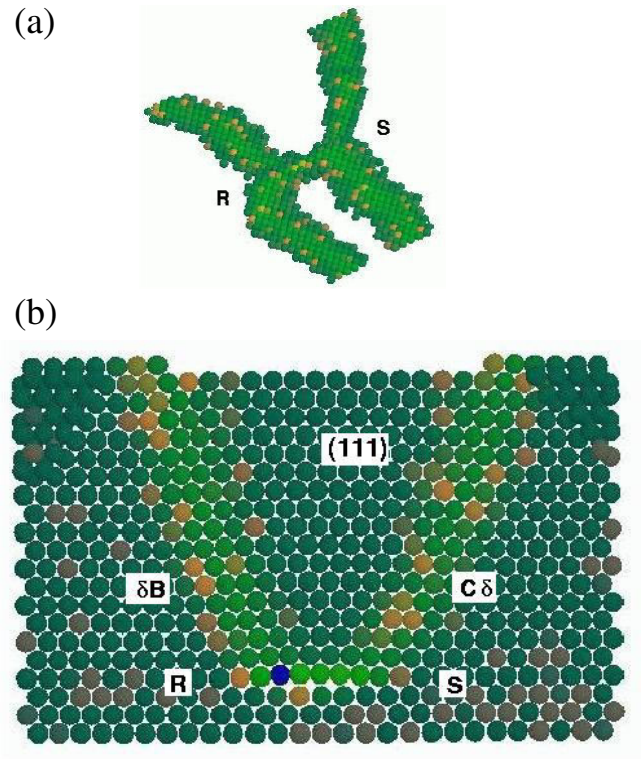

Figure 4. Intersection between screw and edge dislocations, (a) an extended jog RS in the intersected edge dislocation $\boldsymbol{CB}$ with no point defects left behind the screw dislocation $\boldsymbol{DC}$ after intersection, (b) the atomic configuration around the extended jog RS in the (111) plane.

The schematic drawing of the extended jog RS shown in figure 2(c) is shown in figure 5(a). The partial $\boldsymbol{B}\delta$ dissociates into $\boldsymbol{B}\alpha + \alpha\delta$ at point R and partial $\alpha\boldsymbol{A}$ into $\delta\alpha + \alpha\boldsymbol{A}$ at point U, resulting in a stair-rod dipole $\delta\alpha$–$\alpha\delta$. The Burger's vectors of the stair-rod dipole are $\pm[110]/6$, the atom spacing along the dipole line is $[1\bar{1}1]/2$ and the normal distance between the step planes containing the dipole lines is $[001]/2$. Thus the vacant volume per atom site is $(\frac{1}{6}[110]a_0 \times \frac{1}{2}[1\bar{1}0]a_0)\frac{1}{2}[001]a_0 = a_0^3/12$. The volume of an atom is $a_0^3/4$ so that the stair-rod dipole $\delta\alpha$–$\alpha\delta$ in the unit jog corresponds to a row of one-third vacancies, which is consistent with the simulation result shown in figure 2(d). The schematic drawing of the extended jog EF shown in figure 3(a) is shown in figure 5(b). A stair-rod dipole $\boldsymbol{AB}/\alpha\beta$–$\delta\beta/\boldsymbol{AB}$ forms and a similar calculation shows that the interstitial volume per atom site in the dipole is also $a_0^3/12$. Therefore, the stair-rod dipole $\boldsymbol{AB}/\alpha\beta$–$\delta\beta/\boldsymbol{AB}$ in the unit jog corresponds to a row of one-third interstitials. The simulation result shown in figure 3(b) indicates only that the jog is of interstitial type. The schematic drawing of the extended jog RS shown in figure 4(a) is shown in figure 5(c). The stair-rod dipole $\delta\alpha$–$\alpha\delta$ also corresponds to a row of one-third vacancies, which is consistent with the simulation result shown in figure 4(b).

A non-conservative motion of a jog line on a moving dislocation creates a trail of vacancies or interstitials behind, which can be determined according to the criterion proposed by Li and Zhou [14]. If $(\boldsymbol{b}_2 \times \boldsymbol{b}_1)\nu < 0$, a row of vacancies will be created, and if $(\boldsymbol{b}_1 \times \boldsymbol{b}_2)\nu > 0$, a row of interstitials will be created, where $\boldsymbol{b}_1$ and $\boldsymbol{b}_2$ are the Burger's vectors of the moving dislocation $\boldsymbol{DC}$ and the intersected dislocation $\boldsymbol{BA}$ or $\boldsymbol{AB}$, respectively, and ν is the direction

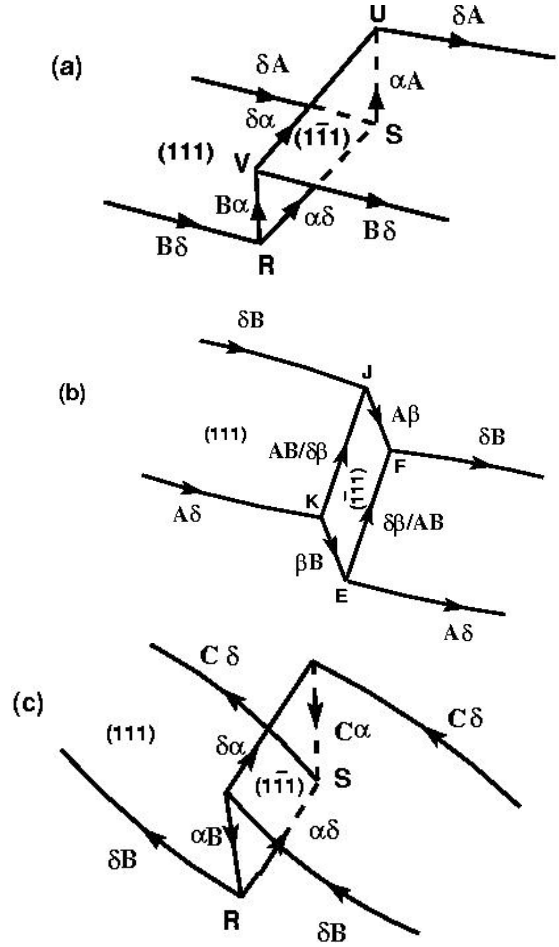

Figure 5. Schematic drawing of extended jogs, (a) RS on the right-hand screw dislocation BA, which corresponds to figure 2(c), (b) EF on the left-hand screw dislocation AB, which corresponds to figure 3(a), (c) RS on the edge dislocation CB, which corresponds to figure 4(a).

of dislocation motion. In this case, $\nu = [\bar{1}12]$. If a moving right-hand screw dislocation $DC = b_1 = [110]/2$ intersects a left-hand screw dislocation $BA = b_2 = [1\bar{1}0]/2$, $(b_2 \times b_1)\nu < 0$, a row of vacancies will be created, as shown in figure 2(d). Conversely, if a right-hand screw dislocation $AB = b_2 = [\bar{1}10]/2$ is intersected by $CD = b_1 = [110]/2$, $(b_2 \times b_1)\nu > 0$, a row of interstitials will be created, as shown in figure 3(b).

4. Conclusions

An extended screw dislocation can recombine into a constriction on the surface through thermal activation at 30 K, resulting in cross-slip at low temperature.

The extended jogs created after intersections of a right-hand screw dislocation with a left-hand and a right-hand one correspond to a row of one-third vacancies and a row of one-third interstitials, respectively.

The intersection between a right-hand screw dislocation and an edge dislocation creates an extended jog corresponding to a row of one-third vacancies.

Acknowledgments

The project was supported by the special Funds for the Major State Basic Research Projects (No G19990650) and by the National Natural Science Foundation of China (50171012).

References

[1] Hirth J P and Lothe J 1982 *Theory of Dislocations* (New York: Wiley)
[2] Balk T J and Hember K J 2001 *Mater. Sci. Eng.* A **309/310** 108
[3] Yonenaga I, Lim S H, Lee C W and Shindo S 2001 *Mater. Sci. Eng.* A **309/310** 125
[4] Yang L H, Soderlind P and Moriarty J A 2001 *Mater. Sci. Eng.* A **309/310** 102
[5] Lu G, Kioussis N, Bulatov V and Kaxiras E 2001 *Mater. Sci. Eng.* A **309/310** 142
[6] Veffe T 2001 *Mater. Sci. Eng.* A **309/310** 113
[7] Li S, Gao K W, Qiao L J, Zhou F X and Chu W Y 2001 *Comput. Mater. Sci.* **20** 143
[8] Bulatorv V, Abraham F F, Kubin L, Devincre B and Yip S 1998 *Nature* **391** 669
[9] Zhou S J, Preston D L, Lomdahl P S and Beazley D M 1998 *Science* **279** 1417
[10] Swaminarayan S, LeSar R, Lomdahl P and Beazley D 1998 *J. Mater. Res.* **13** 3478
[11] Gumbsch P and Gao H 1999 *Science* **283** 965
[12] Johnson R A 1988 *Phys. Rev.* B **37** 3924
[13] Rapaport D C 1995 *The Art of Molecular Dynamics Simulation* (Cambridge: Cambridge University Press)
[14] Li M and Zhou S J 1999 *Phil. Mag. Lett.* **79** 773